Journal of Comparative Physiology B (2021) 191:731–740
https://doi.org/10.1007/s00360-021-01356-y

ORIGINAL PAPER

Osmoregulatory plasticity during hypersaline acclimation in red drum, *Sciaenops ocellatus*

Leighann Martin[1] · **Andrew J. Esbaugh**[1]

Received: 6 June 2020 / Revised: 3 February 2021 / Accepted: 17 February 2021 / Published online: 12 April 2021

Abstract

Prolonged drought and freshwater diversion are making periods of hypersalinity more common in coastal ecosystems. This is especially true in the Laguna Madre system along the Texas coast where salinities can exceed 60 g/kg. As such, the ability to tolerate hypersalinity is critical to the success of endemic species, such as the commercially important red drum (*Sciaenops ocellatus*). This study evaluated acclimation of red drum to hypersalinity (60 g/kg) using a direct transfer protocol. Hypersalinity exposure resulted in significant impacts on plasma osmolality and muscle water in the first 24 h, but returned to control values coincident with a significant increase in intestinal water volume. Hypersalinity acclimation resulted in significant branchial and intestinal plasticity. The gill showed significant elevated *nka α1a, nkcc1* and *vha* (B subunit) mRNA abundance, as well as NKA enzyme activity. The posterior intestine showed a stronger plasticity signal than the anterior intestine, which included a 12-fold increase in *nkcc2* mRNA abundance and significant increases in NKA and VHA enzyme activity. These changes were corroborated by a significant threefold increase in bumetanide-sensitive absorptive short circuit current. These data suggest that the dynamic regulation of NKCC2-mediated intestinal water absorption is an important compliment to HCO_3^--mediated water absorption during hypersalinity exposure and acclimation.

Keywords Osmoregulation · Salinity transfer · Na^+ K^+ ATPase · V-type ATPase · NKCC · Hypersalinity

Introduction

The southern coast of Texas is home to the longest barrier island in the world, Padre Island, which runs almost 200 km. This island, along with the smaller barrier islands to the north, contributes to an expansive network of lagoons and estuaries that have limited capacity for water exchange with the Gulf of Mexico. Furthermore, the limited riverine input and shallow depths of this system combine with high summer temperatures and periodic drought to create a hypersaline environment that can exceed 60 g/kg (Wilson and Dunton 2018). Yet, the estuaries and lagoons of this system are known to act as important habitat for many recreationally and commercially important fisheries (Rooker et al. 2010; Carson et al. 2014). One such species is the red drum (*Sciaenops ocellatus*). This popular sportfish spawns in the coastal oceans near channels that enter estuaries, and the fertilized embryos are carried into the estuary via tidal currents. Larvae subsequently settle to seagrass beds and utilize the estuarine habitat as a nursery ground for approximately three years before leaving the estuary to join the adult spawning population (Holt et al. 1983; Rooker et al. 1998; Stunz et al. 2002). While studies have explored the physiological mechanisms that allow this species to transition between freshwater and seawater environments (Watson et al. 2014; Esbaugh and Cutler 2016), we are unaware of any work addressing their ability to acclimate to the hypersaline environments found along the western coast of the Gulf of Mexico.

Marine fish offset diffusive water loss by drinking and absorbing seawater (reviewed by Grosell 2011). This begins with esophageal desalinization where 50% of the salts are absorbed across the water-impermeable epithelium, which lowers osmotic pressure to approximately that of the plasma (Hirano and Mayer-Gostan 1976; Parmelee and Renfro 1983; Esbaugh and Grosell 2014). As fluid enters the water permeable intestine, additional ions are absorbed which drives water uptake. Excess salts are subsequently excreted at the

Communicated by B. Pelster.

✉ Leighann Martin
leighann.martin@utexas.edu

[1] Department of Marine Science, Marine Science Institutem, University of Texas at Austin, Port Aransas, TX 78373, USA

gills, resulting in net water uptake. There are two general pathways for intestinal ion absorption: HCO_3^--dependent, and HCO_3^--independent. The former refers to the secretion of HCO_3^- across the apical membrane in exchange for Cl^-, which occurs via the slc26a6 exchanger (Grosell et al., 2009a). The required HCO_3^- is either produced from metabolic CO_2 via carbonic anhydrase (CA) (Sattin et al., 2010), or taken from the plasma via the basolateral Na^+ HCO_3^- co-transporter (NBC) (Kurita et al., 2008; Taylor et al., 2010). The HCO_3^--independent pathway refers to the electroneutral uptake of Na^+ and Cl^-, which in red drum occurs through the Na^+ K^+ Cl^- co-transporter 2 (NKCC2 (Esbaugh and Cutler 2016). Both of these pathways are powered by basolateral Na^+ K^+ ATPase (NKA) (Grosell and Genz 2006; Esbaugh and Cutler 2016), while HCO_3^- secretion also incorporates apical V-type H^+ ATPase (VHA) (Grosell et al. 2009b; Guffey et al. 2011).

In general, fish that transition from seawater to extreme hypersaline habitats must maximize the pathways already in place for intestinal water absorption and branchial ion excretion (see reviews Gonzalez 2012; Laverty and Skadhauge 2012). While esophageal desalination has not been shown to exhibit plasticity in response to hypersalinity (i.e. ≥ 60 g/kg) (Esbaugh and Grosell 2014), the intestine has been shown to exhibit plasticity in Gulf toadfish (*Opsanus* beta) as evident from a doubling of rectal base excretion rates (Taylor et al. 2010). Numerous mechanisms have been implicated in this process, including up-regulation of VHA (Guffey et al. 2011) and CA (Sattin et al. 2010) in the posterior intestine, as well as an up-regulation of NBC observed only in the mid-intestine (Taylor et al. 2010). Interestingly, we are unaware of any examination of intestinal NKCC2, which has been implicated in freshwater to seawater transitions in red drum (Esbaugh and Cutler 2016). For the gill, the available evidence suggests that fish increase the abundance of several proteins involved in normal Na^+ Cl^- excretion. These include: elevated NKA activity and mRNA abundance (Gonzalez 2012; Lorin-Nebel et al. 2012; Li et al. 2014; Lema et al. 2018; Malakpour Kolbadinezhad et al. 2018); elevated CFTR mRNA (Li et al. 2014; Marshall et al. 2018) and distribution (Cozzi et al. 2015); elevated claudin-10c, -10e and -10f isoform mRNA, which act to maintain cation pore selectivity in the tight junction between ionocytes and accessory cells (Marshall et al. 2018). Overall, these changes are thought to enable fish exposed to hypersalinity to generate electrochemical gradients that exceed the higher equilibrium potentials found in hypersaline environments (e.g. Sardella et al. 2004; Gonzalez et al. 2005; Cozzi et al. 2015).

On this background, we sought to identify the osmoregulatory consequences and recovery patterns, as well as physiological plasticity in the gills and intestine of marine fish acutely exposed to 60 g/kg salinity. We assessed organismal osmoregulatory status following direct transfer from 30 to 60 g/kg using plasma ion chemistry, muscle water and quantification of intestinal fluid. We assessed plasticity in the gills and intestines using a combination of enzyme assays, relative mRNA quantification, and isolated tissue Ussing chamber preparations.

Materials and methods

Experimental fish

All experiments were performed with the approval from the University of Texas at Austin's Institutional Animal Care and Use Committee (IACUC). Juvenile red drum (*Sciaenops ocellatus*) was obtained from Ekstrom Aquaculture LLC (Palacios, TX, USA) in the fall of 2015 and reared in seawater (30 g/kg). Fish were housed on-site at the Fisheries and Mariculture Laboratory (FAML) at the University of Texas Marine Science Institute (Port Aransas, TX, USA). Fish were kept in a recirculating system with sterilized seawater (30 g/kg,) originating from the Corpus Christi ship channel. Water quality was monitored daily for ammonia (> 0.25 mg/l) and weekly for pH (7.8 to 8.0). A 25% water change was performed weekly. All fish were held in tanks maintained at 22 °C with constant aeration. Fish were fed AquaMax sportfish feed (Purina, USA) daily to satiation but were starved for at least 48 h prior to tissue sampling.

Experimental protocol

Isolated exposures were performed in 5-L tanks that were filled with either 30 g/kg seawater or seawater supplemented with artificial sea salts (Instant Ocean, Spectrum Brands, Blacksburg, VA, USA) to a final salinity of 60 g/kg. Water chemistry was determined in the same manner as the seawater holding tanks. An isolated fish ($N = 48$; 58.7 ± 0.97 g; mean ± SEM) was transferred to either seawater or hypersalinity directly from the seawater holding tanks. Seawater controls were sampled directly from the holding tanks (0 h) or 168 h after transfer ($N = 8$ each), while hypersalinity fish were sampled at 4, 24, 72, and 168 h ($N = 8$ each). To ensure that handling had no effect, a secondary experiment ($N = 12$; 43.8 ± 2.3 g; mean ± SEM) was performed for seawater transfer controls and sampled at 4, 24, and 72 h ($N = 4$ each). For the Ussing chamber experiments, fish ($N = 12$; 121.7 ± 18.4 g; mean ± SEM) were transferred from the general seawater holding tanks into 200 gallon tanks at either 30 or 60 g/kg ($N = 6$ each). Posterior intestine was sampled 72 h after transfer.

Tissue collection

Fish were euthanized by immersion in MS-222 (250 mg/L buffered with $NaHCO_3$) followed by spinal transection. Blood was sampled via caudal puncture and plasma was separated by centrifugation (1 min at 10,000*g*, 4 °C). A ventral incision was made to expose the abdominal cavity and clamps were placed after the pyloric ceca and before the rectum to isolate intestinal fluid. The intestine was then excised, and the fluid was drained into a pre-weighed tube. The anterior (first third) and posterior (final third) intestines were dissected, and both sections were divided in half for enzyme and real-time PCR analysis. Gill lamellae were dissected from both sides of animal with one side being used for real-time PCR and the other for enzyme analysis. All tissue samples were flash-frozen using dry ice and stored at -80 °C. White muscle was removed from the dorsal side of the body and immediately processed for muscle water content.

Osmolyte and biochemical analysis

Intestinal fluid contents were centrifuged for 15 min at 10,000*g* to pellet organic material and $CaCO_3$ precipitates. The fluid supernatant was removed, and the volume was determined gravimetrically. The plasma osmolality was determined using a VAPRO 5520 osmometer (Wescor, Logan, UT, USA). The white muscle tissue was weighed and placed in a dehydrating oven at 60 °C. The tissue samples were weighed daily until measurements were consistent for three consecutive days. Muscle water was calculated as the wet weight minus the final dry weight, which was subsequently divided by the wet weight to obtain percent muscle water. Standard protocols were employed to determine branchial and intestinal NKA and VHA activity (Lin and Randall 1993; McCormick 1993) using ouabain and N-ethymaleimide as selective inhibitors, respectively. Note that activity was only assessed at control and 72 h post-transfer time points. Enzyme activities were normalized to total protein content, as determined using a Bradford assay.

mRNA analysis

All described methods were performed in accordance to manufacturer guidelines unless otherwise stated. Total RNA was extracted using TRI Reagent (Molecular Research Center Inc, Cincinnati, USA). Total RNA was quantified using an ND-1000 spectrophotometer (Thermo Scientific, USA) at a wavelength of 260 nm and sample purity was assessed using 260:280 ratios. A 1 µg sample of RNA was DNase-treated with amplification grade DNase I (Thermo Scientific, USA) to remove potential DNA contamination. The resulting DNase-treated RNA was reverse-transcribed using RevertAid (Thermo Scientific, USA). Real-time PCR was performed on an Mx3000P real-time PCR system (Stratagene, La Jolla, CA, USA) using the Maxima SYBR green master mix kit (Thermo Scientific, USA; 12.5 µL reactions). Dissociation curves were also used to assess the primer specificity of each reaction during the real-time PCR run. Relative mRNA abundance was calculated using the delta-delta ct method (Pfaffl 2001) using elongation factor 1α (ef1α) as an internal control and the time zero seawater controls as the relative control, refer to Table 1 for primer sequences. Successful DNase treatment was verified using a no-reverse transcriptase control. Primer sets for *nka* (α1-subunit) were designed using the Primer3 freeware and specificity was verified using standard PCR and gel electrophoresis. The other primer sets have been previously validated for red drum and published as follows: *ef1α, cftr, nkcc1, nkcc2* (Watson et al. 2014), *CA-c, nbc, vha* (β-subunit) (Allmon and Esbaugh 2017), *slc26a3a,* and *slc26a6* (Esbaugh and Cutler 2016). The sample size for mRNA analysis, after accounting for RNA purification and quality, is as follows: Gill: 0 h = 8, 4 h = 7, 24 h = 7, 72 h = 6; Anterior Intestine: 0 h = 8, 4 h = 8, 24 h = 8, 72 h = 8; Posterior Intestine: 0 h = 8, 4 h = 7, 24 h = 6, 72 h = 7.

Electrophysiology

Electrophysiological recordings were performed on the end of an isolated posterior intestine epithelia as previously described (Esbaugh and Cutler 2016). Briefly, the posterior intestine of fasted animals (48 h) acclimated to control or hypersalinity (72 h) was dissected and immediately mounted in a 0.4 cm^2 surface area tissue holder that was placed between two Ussing half chambers (Physiologic Instruments, San Diego, CA, USA.). Each chamber contained 2 ml of serosal style saline: 151 mM NaCl, 3 mM KCl, 0.88 mM $MgSO_4$, 5 mM $NaHCO_3$, 1 mM $CaCl_2$, 0.5 mM NaH_2PO_4, 0.5 mM KH_2PO_4, 4.5 mM urea, 5 mM glucose, 3 mM HEPES (Na^+ salt), 3 mM HEPES (free acid), pH = 7.8. Temperature was maintained at 25 °C by a recirculating water bath and both chambers were aerated by a 0.3% CO_2 in O_2 mixture. Saline was aerated for at least 60 min prior to experimentation. Short circuit current (I_{sc}) was measured under symmetrical voltage clamp conditions using current and voltage electrodes (Physiologic Instruments, San Diego, CA, USA.; P2020-S) connected to an amplifier (Physiologic Instruments, San Diego, CA, USA.; VCC600). Electrode tips contained 3% agar solution and 3 M KCl. Conductance of the epithelium was determined by passing 3 s pulses of 1 mV from mucosal to serosal bath every 60 s. To inhibit NKCC activity, a final concentration of 10 µM bumetanide, or 0.1% DMSO vehicle control, was

Table 1 List of primers used for real-time PCR

Gene	Accession #	Orientation	Sequence
ef1a	KJ958539	F	GTTGCTGGATGTCCTGCACG
		R	GTCCGTGACATGAGGCAGACTG
nkcc1	KJ958543	F	GCGATAAGGCAACTCCCACC
		R	CGCGAAGTTCACCACCCGAA
nkcc2	KJ958544	F	GGAGCGATCTCTGTGCCAGAC
		R	ACCAGGACACCCCTGATCCA
nka a1a	MN483062	F	GTCATCAACACTGGAGACCGTA
		R	GTGATGATGTGGATGAAGTGCT
vha B subunit	KU899108	F	CCTACCATTGAGCGTATCATCA
		R	CGTAGGAGCTCATGTCAGTCAG
slc26a3a	KX507131	F	CAACTGTTGCTTCTTTGACGAC
		R	AGTCTGGGTGTTTCTCGATGAT
slc26A6	KX507133	F	TGCCAGGGATTTTGATCTTC
		R	GTTTCTTCTTTGCCGACAGG
CAc	KM387716	F	TGACATTCGCAGACGACTCCGA
		R	AGCAGGATACTTGGTCCCTTCCA
nbc	KM387714.1	F	TCTTCATCTACGACGCTTTCAA
		R	TCATATTGAGTGACGAGGTTGG
cftr	KJ958542	F	GACCCTGAAGCTGTCCAGCAG
		R	GGTGATCCATACAAAGTGGGCCA

All sequences are 5′–3′ and reverse primers are compliments of the genetic sequence

added to the mucosal saline bath after stable control values had been obtained (Esbaugh and Cutler 2016). In all cases, the effects of bumetanide were apparent within minutes, but tissues were allowed to stabilize for final determinations. In all cases, reported data represent the average of a stabilized tissue over 20 min.

Statistical analysis

Plasma osmolality, intestinal fluid, muscle water and relative mRNA abundance were analyzed using a one-way analysis of variance (ANOVA). Relative mRNA abundance was natural log-transformed prior to statistical analysis. ATPase activity was assessed using a student's t test. Assumption for normality was tested using a Shapiro–Wilk test and the assumption of equal variance was assessed using a Brown–Forsythe test. A non-parametric ANOVA on ranks was performed in cases where assumptions were not met. Electrophysiological data were assessed using a repeated measures two-way ANOVA with salinity treatment as a non-repeating factor and inhibitor treatment as a repeating factor. All statistical significance is based on $P \leq 0.05$, and SigmaPlot 13 (SyStat Software Inc, San Jose, CA, USA.) was used for all analysis.

Results

Fluid and muscle osmolytes

Red drum transferred from seawater (30 g/kg) to hypersalinity (60 g/kg) showed a significant increase in plasma osmolality by 4 h (Fig. 1a), with recovery to control levels by 72 h post transfer. Muscle water significantly decreased at 4 and 24 h post transfer (Fig. 1b), but also recovered to control by 72 h. Transfer to hypersalinity was also associated with a significant increase in intestinal fluid volume at all time points (Fig. 1c). Note that no significant differences for any variable were observed between 0, 4, 24, 78 and 168 h control fish (Fig. 1; Table 2). These analyses indicate that red drum was fully acclimated to acute hypersalinity transfer by 72 h, and as such further assessment of phenotypic plasticity was restricted to this window.

Branchial plasticity

Red drum acutely transferred to hypersalinity exhibited significantly increased relative mRNA abundance of branchial *nkcc1* and *nka* at 4, 24 and 72 h post transfer. Transcript abundance of *vha* showed a significant increase at only 4 h (Fig. 2). There was also a trend toward elevated *cftr* mRNA, although this was just outside of statistical significance (ANOVA on Ranks; $P = 0.051$). The elevated

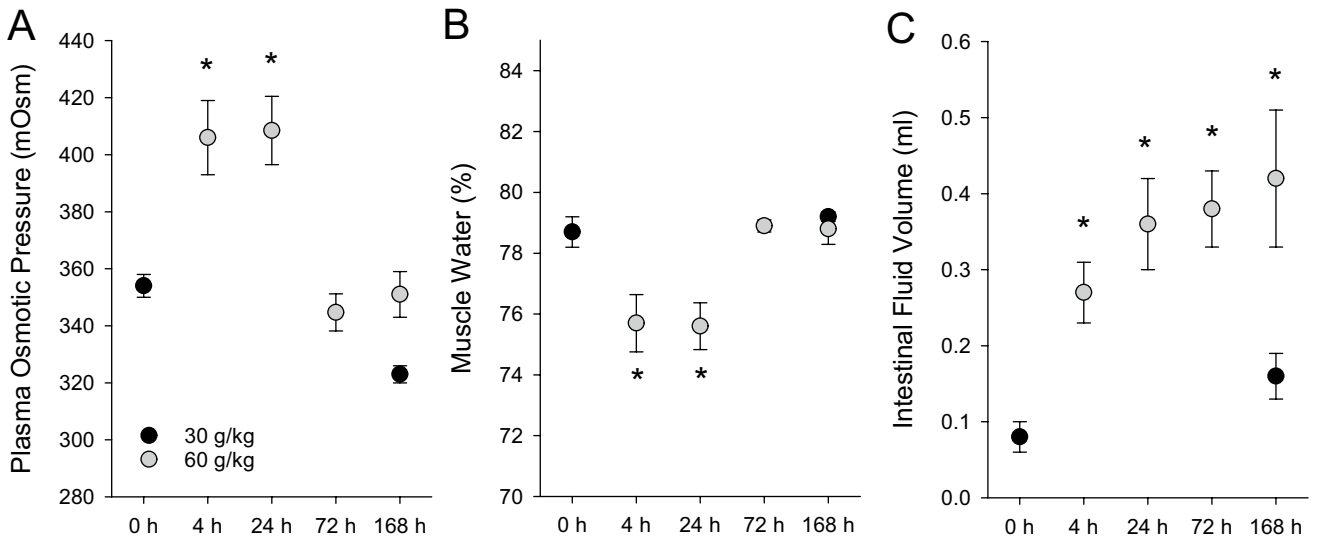

Fig. 1 Plasma osmolality (**a**), muscle water content (**b**), and intestinal fluid content (**c**) following transfer from seawater (30 g/kg) to hypersaline water (60 g/kg) in red drum (*Sciaenops ocellatus*). Significant differences from the seawater acclimated (0 h) time point are denoted by an asterisk ($P \leq 0.05$; $N = 8$)

Table 2 Secondary control time points ($N = 12$; 43.8 ± 2.3; mean ± SEM)

Control time point	Plasma osmolality (mOsm)	Muscle water content (%)	Intestinal fluid content (g)
4 h	326.0 ± 2.48	78.87 ± 0.19	0.22 ± 0.04
24 h	328.0 ± 2.45	78.95 ± 0.14	0.08 ± 0.02
72 h	329.4 ± 4.01	79.41 ± 0.34	0.11 ± 0.03

No shown effect of transfer from holding tank to seawater in the plasma osmolality, muscle water content, or intestinal fluid content

relative mRNA abundance of *nka* and *vha* was validated at the phenotype level for NKA using enzymatic activity, which demonstrated significantly increased activity 72 h post transfer. While a similar trend was observed VHA activity, it was outside of statistical significance ($P = 0.14$; Student's *t* test). The NKA activity was threefold higher at the point of acclimation compared to control, while VHA was approximately double (Fig. 3a).

Intestinal plasticity

The anterior intestine showed a small but significant increase in *nkcc2* relative mRNA abundance after 4 h, while *nka* relative mRNA was significantly increased at all time points compared to the control. Transcript abundance of *vha* was increased at 4 h and 72 h. No changes in relative mRNA were observed for *slc26a3*, *slc26a6*, *nbc*, *or CA-c* post-transfer. In fact, the *slc26a6* exhibited reduced relative abundance at 4 h, and *CA-c* showed decreased relative abundance at 24 h

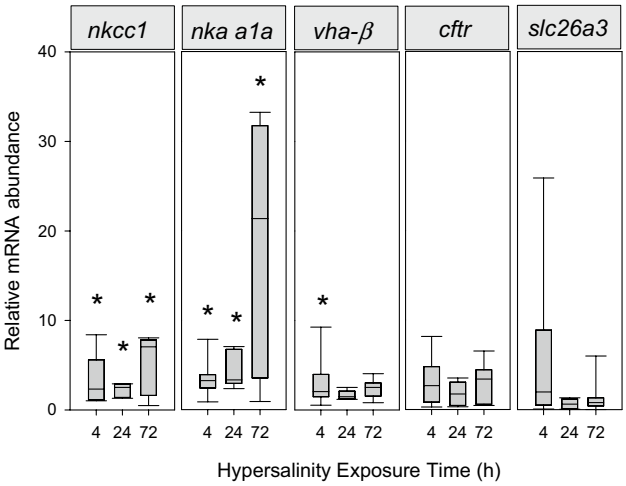

Fig. 2 Relative transcript abundance for osmoregulatory proteins in the gills of red drum (*Sciaenops ocellatus*) following acute hypersaline transfer. All mRNA abundance values are expressed relative to the abundance elongation factor 1α mRNA and normalized to the seawater acclimated treatment (0 h = 1). Boxes represent the 25th through 75th quartile data with the median represented by the central line. The whiskers represent the maximum and minimum observed data. Significant differences from seawater fish are denoted by an asterisk ($P \leq 0.05$; $N = 8$)

(Fig. 4). The anterior intestine showed no significant differences in NKA or VHA enzyme activity at 72 h post transfer (Fig. 3b). The posterior intestine exhibited a significantly elevated mRNA abundance of 12-fold for *nkcc2* at 4 h. As in the anterior intestine, *slc26a6* mRNA was significantly lower at 4 h and 72 h, while *slc26a3* showed elevated mRNA

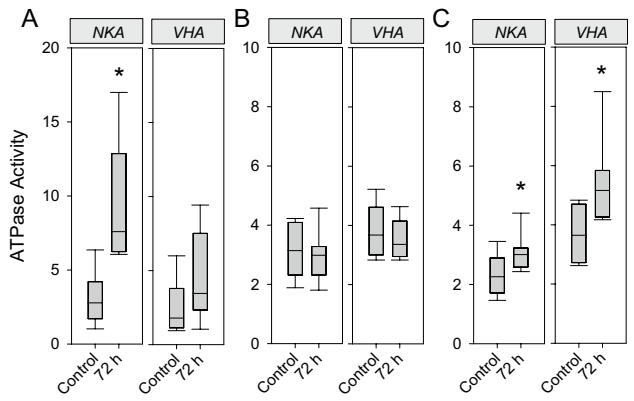

Fig. 3 Na^+ K^+ ATPase and V-type H^+ ATPase enzyme activity (μmol/mg protein/h) in the **a** gill, **b** anterior intestine, and **c** posterior intestine following 72 h of hypersaline exposure. Boxes represent the 25th through 75th quartile data with the median represented by the central line. The whiskers represent the maximum and minimum observed data. Significant differences from seawater acclimated fish are denoted by an asterisk ($P \leq 0.05$; $N = 8$)

at 72 h (Fig. 5). The posterior intestine showed significantly increased enzyme activity for both NKA and VHA at 72 h post transfer (Fig. 3c).

Electrophysiology

A final organ level phenotypic assessment was performed on the posterior intestine using an Ussing chamber. Consistent with the mRNA and enzyme analysis, the hypersaline acclimated individuals had a more absorptive epithelia under symmetrical conditions as evidenced by a significantly higher I_{sc} (Fig. 6). Addition of bumetanide—a selective *nkcc* inhibitor—resulted in a significant reduction in I_{sc} in both control and hypersaline acclimated fish. There was no significant interaction ($P = 0.395$) between acclimation and bumetanide exposure, which demonstrated that the magnitude of inhibition was similar between the two acclimation groups. There was no effect of salinity or bumetanide treatment on epithelial conductance (data not shown). The mean epithelial conductance for the four treatments is (mS cm^{-2}): 35 g/kg—control = 10.8 ± 0.8; 35 g/kg—bumetanide = 12.1 ± 0.7; 60 g/kg—control = 11.2 ± 1.0; 60 g/kg—bumetanide = 14.3 ± 1.3.

Discussion

The results of this study demonstrate that red drum can quickly acclimate to hypersalinity to restore extracellular and intracellular osmoregulatory variables to control levels. While evidence indicates that behavioral responses (e.g. drinking rate) are involved in this process, our data also demonstrate gill and intestinal plasticity that is consistent with elevated osmoregulatory capacity. Importantly, the mechanisms of plasticity also suggest that hypersalinity exposure and acclimation will increase the energetic costs of osmoregulation, which raises further questions regarding the whole animal consequences of hypersalinity exposure.

Three variables were selected as indicators of whole animal osmoregulatory status: (1) plasma osmolality, (2) muscle water, and (3) intestinal fluid volume. Plasma osmolality and muscle water showed a significant increase and decrease, respectively, at 4 and 24 h post transfer after which both returned to control levels (Fig. 1a). This is consistent with an initial osmotic insult that is quickly corrected. For comparison, the Gulf toadfish (*Opsanus*

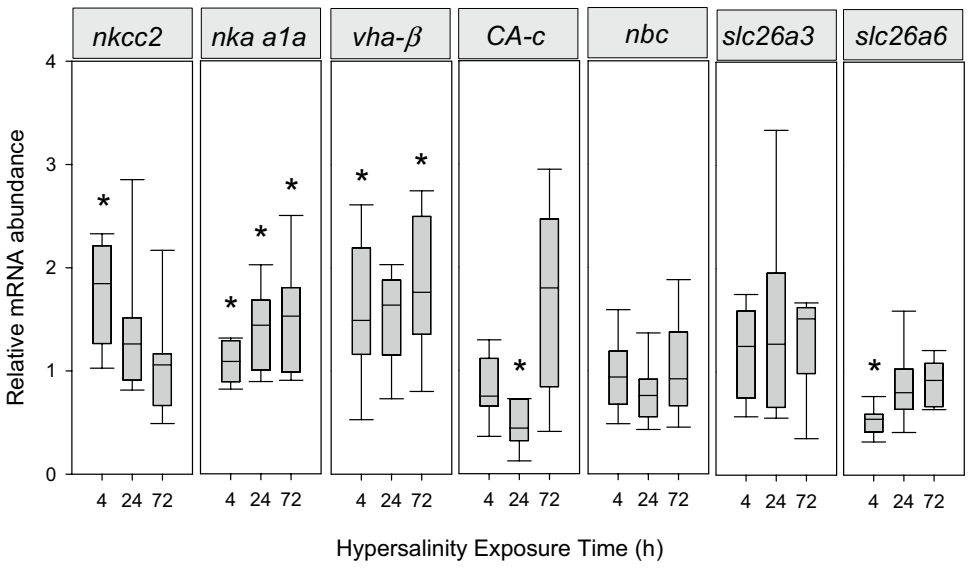

Fig. 4 Relative transcript abundance for osmoregulatory proteins in the anterior intestine of red drum (*Sciaenops ocellatus*) following acute hypersaline transfer. All mRNA abundance values are expressed relative to the abundance elongation factor 1α mRNA and normalized to the seawater acclimated treatment (0 h = 1). Boxes represent the 25th through 75th quartile data with the median represented by the central line. The whiskers represent the maximum and minimum observed data. Significant differences from seawater fish are denoted by an asterisk ($P \leq 0.05$; $N = 8$)

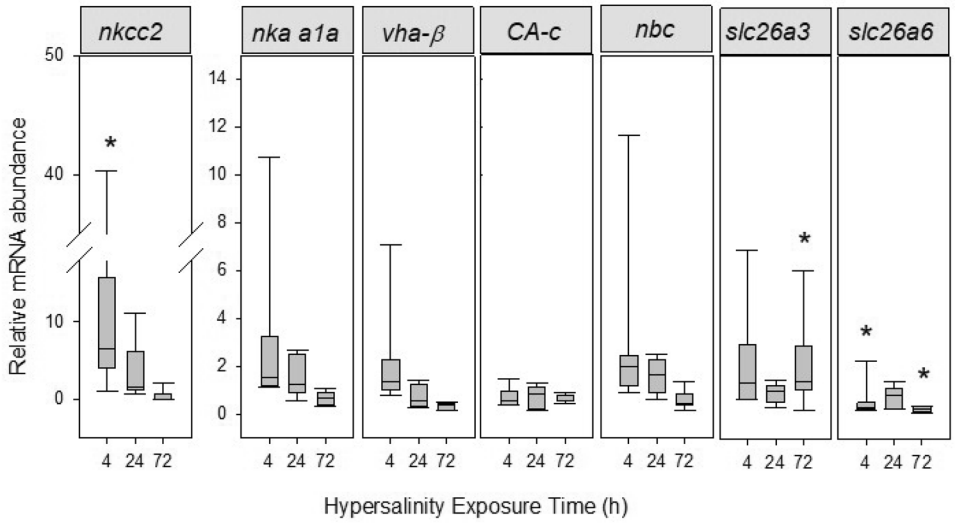

Fig. 5 Relative transcript abundance for osmoregulatory proteins in the posterior intestine of red drum (*Sciaenops ocellatus*) following acute hypersaline transfer. All mRNA abundance values are expressed relative to the abundance elongation factor 1α mRNA and normalized to the seawater acclimated treatment (0 h = 1). Boxes represent the 25th through 75th quartile data with the median represented by the central line. The whiskers represent the maximum and minimum observed data. Significant differences from seawater fish are denoted by an asterisk ($P \leq 0.05$; $N = 8$)

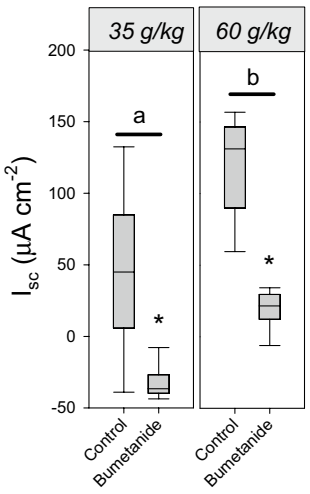

Fig. 6 Short circuit current (I_{sc}) measured from the posterior intestine of red drum (*Sciaenops ocellatus*) following 72-h hypersaline transfer. Boxes represent the 25th through 75th quartile data with the median represented by the central line. The whiskers represent the maximum and minimum observed data. Letters denote significant differences between acclimation groups, and asterisks denote significant inhibition by 10 μM bumetanide ($P \leq 0.05$; $N = 6$). There was no significant interaction between acclimation and bumetanide treatment ($P = 0.39$)

beta) exhibited a significant increase in plasma osmolality and intestinal volume at 24 h post transfer to 70 g/kg (Genz et al. 2011), but these variables did not return to control values even after 7 days (McDonald and Grosell 2006). Tilapia hybrids (*Oreochromis mossambicus* × *O. urolepis hornorum*) showed elevated plasma osmolality after 24 h of exposure to 65 g/kg, which was recovered by 120 h post transfer (Sardella et al. 2004). Amargosa pupfish (*Cyprinodon nevadensis amargosae*) showed elevated plasma osmolality after 4 days in 55 g/kg versus seawater acclimated fish, which was fully recovered by 14 days post transfer (Lema et al. 2018). *Fundulus heteroclitus* did not exhibit an elevated plasma osmolality until 3 days post transfer to double-strength seawater, and this returned to control values by 10 days post transfer (Marshall et al. 2018). Overall, the onset of osmotic disturbances in red drum is in line with previous work; however, the recovery of these variables by 72 h is somewhat faster than that described for many fishes. The time course of recovery described for red drum is also similar to that previously described following hypo-osmotic (Watson et al. 2014) and hyper-osmotic (Esbaugh and Cutler 2016) stress coinciding with seawater–freshwater transitions.

The observed increase in plasma intestinal volume suggests that red drum drinking rate was quickly (4 h post transfer) elevated following hypersalinity transfer. This is a faster response than previously described for red drum when transitioning from freshwater to seawater, which did not show increased intestinal fluid volume until 72 h post transfer (Esbaugh and Cutler, 2016). Nonetheless, this response is consistent with previously described drinking patterns following hyperosmotic stress in fishes (Lin et al. 2001; McDonald and Grosell 2006; Scott et al. 2008). Yet, the more interesting finding relates to the plasticity of the intestinal epithelium following hypersalinity transfer. Both the anterior and posterior intestines showed significant up-regulation of *nkcc2* by 4 h post transfer, with additional up-regulation of *nka* and *vha* subunits in the anterior intestine. Yet, the enzymatic activities of both ATPases were only elevated in the posterior section of the intestine. The significance of these mRNA and biochemical changes in the posterior intestine was demonstrated by a threefold increase in I_{sc} following 72 h of acclimation to 60 g/kg salinity. As expected, this current was significantly inhibited by bumetanide, verifying the role of apical NKCC. Interestingly, the hypersaline

acclimated tissue maintained an absorptive current following bumetanide addition, while the control tissue exhibited a secretory current. It is unclear if this is an indication of non-NKCC apical transport that may contribute to an absorptive I_{sc}, or if it is simply due to incomplete inhibition of NKCC. In either case, these results fit well with prior work on Mozambique tilapia and Gulf toadfish that have reported elevated *nkcc2* mRNA concentration (Li et al. 2014) and elevated protein abundance (Schauer et al. 2018), respectively, following hypersalinity acclimation. Similar intestinal plasticity was also observed in red drum when transitioning from freshwater to seawater (Esbaugh and Cutler 2016), with the exception that those observations were from the anterior intestine and that the observed I_{sc} was much lower (30 μA/cm^2).

While the observed increase in bicarbonate-independent water absorption pathways agrees with prior work (Li et al. 2014; Esbaugh and Cutler 2016; Schauer et al. 2018), we were surprised by the lack of plasticity in the bicarbonate-dependent water absorption pathway. For example, sea bream (*Sparus aurata*) (Gregório et al. 2013) and Gulf toadfish (Guffey et al. 2011) acclimated to hypersalinity had significantly higher net base secretion rates in the anterior and posterior intestine, respectively. In Gulf toadfish, this was partly attributed to increased VHA activity (Guffey et al. 2011). While the elevated VHA activity was observed in red drum, no changes in *CA-c* and *nbc* mRNA abundance were observed, and *slc26a6* showed only a transient decrease in mRNA abundance following hypersalinity transfer. Both *CA-c* and *nbc* have been shown to increase in mRNA abundance following hypersalinity acclimation in Gulf toadfish (Sattin et al. 2010; Taylor et al. 2010), and *slc26a6* mRNA abundance was elevated in the anterior intestine of sea bream (Gregório et al. 2013). We did observe increased *slc26a3* mRNA abundance at 72 h post exposure in the posterior intestine, which may suggest a role in a slower acclimation response.

While we acknowledge that our data cannot inform on the relative contribution of the bicarbonate-dependent and -independent pathways in driving water absorption, it is safe to conclude that the latter seems to play a much more important role in acute hyperosmotic stress. We theorize that during hypersalinity stress, the intestinal fluid contains a greater concentration of ions that naturally increase the rate of HCO_3^- secretion into the intestinal lumen, which results in elevated fluid HCO_3^- concentrations. This is supported by previous work that has demonstrated fluid concentrations between 60 and 100 mM when exposed to hypersaline environments (McDonald and Grosell 2006; Gregório et al. 2013). This concentration may approach or exceed the thermodynamic limitations on HCO_3^- secretion through *slc26a6*, resulting in an important role for the NKCC2 pathway in augmenting water absorption. Interestingly, the increase in VHA enzyme activity, which is known to be apically oriented in fish intestines, (Guffey et al.2011; Esbaugh and Cutler 2016) is consistent with this theory, as VHA would act to offset the thermodynamic constraints on *slc26a6*.

With respect to the gill, our results generally conform to expectations with the possible exception of the *cftr* mRNA responses. We observed a significant increase in *nkcc1* and *nka a1a* mRNA at all hypersalinity time points, as well as a significant increase in *vha β sub-unit* mRNA at the 4 h post-transfer time point. The NKA mRNA patterns were supported by significantly elevated NKA in the gills at 72 h post transfer. The VHA activity also showed an increasing trend, but was outside the fiducial level of significance. The *cftr* mRNA was not significantly altered by hypersalinity exposure, although again the general trend was in the direction of increased abundance. This was surprising owing to the known role of *cftr* in branchial Na^+ and Cl^- excretion, as well as the fact we have previously been demonstrated dynamic *cftr* mRNA regulation in response to seawater–freshwater transitions in red drum (Watson et al. 2014; Esbaugh and Cutler 2016). The overall pattern described here for branchial plasticity following hypersalinity exposure is similar to that described for Amargosa pupfish (*Cyprinodon nevadensis amargosae*), which also showed significantly elevated *nkcc1* and *nka* mRNA in hypersaline acclimations as compared to seawater acclimations, with no difference in *cftr* mRNA abundance (Lema et al. 2018). In contrast, both killifish (*Fundulus heteroclitus*) and Mozambique tilapia (*Oreochromis mossambicus*) showed significant increases in *cftr* while *nkcc1* remained unchanged between seawater and hypersaline fishes (Li et al. 2014; Marshall et al. 2018). While the reason for these different patterns is unclear, it seems reasonable to hypothesize that it simply represents a difference in the rate limiting proteins for salt excretion between the various species.

In conclusion, our results show that red drum is capable of correcting the osmotic disturbances caused by acute exposure to 60 g/kg within 3 days of transfer. Our results also demonstrate that hypersalinity exposure stimulates osmoregulatory plasticity in the posterior intestine that significantly increases the capacity for transepithelial active transport. These changes in the posterior intestine coincide with significantly increased NKA and VHA activity, as well as *nkcc2* mRNA abundance, which suggests that bicarbonate-independent water absorption plays a particularly important role following transitions into hypersaline environments. Finally, we show that hypersalinity also stimulates increased NKA activity and mRNA abundance, as well as increased *nkcc1* mRNA abundance in the gills, which presumably increases the capacity for branchial ion excretion.

Acknowledgements This work was funded in part by the National Science Foundation (EF1315290). We would like to thank Elizabeth B. Allmon for her help with animal maintenance, sample processing and general oversight.

References

Allmon EB, Esbaugh AJ (2017) Carbon dioxide induced plasticity of branchial acid-base pathways in an estuarine teleost. Sci Rep 7:45680

Carson EW, Bumguardner BW, Fisher M, Saillant E, Gold JR (2014) Spatial and temporal variation in recovery of hatchery-released red drum (Sciaenops ocellatus) in stock enhancement of Texas bays and estuaries. Fish Res 151:191–198

Cozzi RRF, Robertson GN, Spieker M, Claus LN, Zaparilla GMM, Garrow KL, Marshall WS (2015) Paracellular pathway remodeling enhances sodium secretion by teleost fish in hypersaline environments. J Exp Biol 218:1259–1269

Esbaugh AJ, Grosell M (2014) Esophageal desalination is mediated by Na^+, H^+ exchanger-2 in the gulf toadfish (*Opsanus beta*). Comp Biochem Physiol 171:57–63

Esbaugh AJ, Cutler B (2016) Intestinal Na^+, K^+, $2Cl^-$ cotransporter 2 plays a crucial role in hyperosmotic transitions of a euryhaline teleost. Physiological reports 4:13028

Genz J, McDonald MD, Grosell M (2011) Concentration of $MgSO_4$ in the intestinal lumen of Opsanus beta limits osmoregulation in response to acute hypersalinity stress. Am J Physiol Regul Integr Comp Physiol 300:R895-909

Gonzalez RJ (2012) The physiology of hyper-salinity tolerance in teleost fish: a review. J Comp Physiol B 182:321–329

Gonzalez RJ, Cooper J, Head D (2005) Physiological responses to hyper-saline waters in sailfin mollies (*Poecilia latipinna*). Comp Biochem Physiol A Mol Integr Physiol 142:397–403

Gregório SF, Carvalho ESM, Encarnação S, Wilson JM, Power DM, Canário AVM, Fuentes J (2013) Adaptation to different salinities exposes functional specialization in the intestine of the sea bream (*Sparus aurata* L.). J Exp Biol 216:470–479

Grosell M (2011) The role of the gastrointestinal tract in salt and water balance. In: Grosell M, Farrell AP, Brauner CJ (eds) Fish physiology: The multifunctional gut of fish, vol 30. Elsevier, London

Grosell M, Genz J (2006) Ouabain-sensitive bicarbonate secretion and acid absorption by the marine teleost fish intestine play a role in osmoregulation. Am J Physiol Regul Integr Comp Physiol 291:R1145-1156

Grosell M, Mager EM, Williams C, Taylor JR (2009a) High rates of HCO_3^- secretion and Cl^- absorption against adverse gradients in the marine teleost intestine: the involvement of an electrogenic anion exchanger and H^+-pump metabolon? J Exp Biol 212:1684–1696

Grosell M, Genz J, Taylor JR, Perry SF, Gilmour KM (2009b) The involvement of H^+-ATPase and carbonic anhydrase in intestinal HCO_3^- secretion in seawater-acclimated rainbow trout. J Exp Biol 212:1940–1948

Guffey S, Esbaugh A, Grosell M (2011) Regulation of apical H^+-ATPase activity and intestinal HCO_3^- secretion in marine fish osmoregulation. Am J Physiol Regul Integr Comp Physiol 301(6):R1682-1691

Hirano T, Mayer-Gostan N (1976) Eel esophagus as an osmoregulatory organ. Proc Natl Acad Sci U S A 73:1348–1350

Holt SA, Kitting CL, Arnold CR (1983) Distribution of young red drums among different sea-grass meadows. Trans Am Fish So 112:267–271

Kurita Y, Nakada T, Kato A, Doi H, Mistry AC, Chang MH, Romero MF, Hirose S (2008) Identification of intestinal bicarbonate transporters involved in formation of carbonate precipitates to stimulate water absorption in marine teleost fish. Am J Physiol Regul Integr Comp Physiol 294:R1402-1412

Laverty G, Skadhauge E (2012) Adaptation of teleosts to very high salinity. Comp Biochem Physiol A 163:1–6

Lema SC, Carvalho PG, Egelston JN, Kelly JT, McCormick SD (2018) Dynamics of gene expression responses for ion transport proteins and aquaporins in the gill of a euryhaline pupfish during freshwater and high-salinity acclimation. Physiol Biochem Zool 91:1148–1171

Li ZJ, Lui EY, Wilson JM, Ip YK, Lin QS, Lam TJ, Lam SH (2014) Expression of key ion transporters in the gill and esophageal-gastrointestinal tract of euryhaline mozambique tilapia *Oreochromis mossambicus* acclimated to fresh water, seawater and hypersaline water. PLoS ONE 9:e87591

Lin H, Randall DJ (1993) H^+-ATPase activity in crude homogenates of fish gill tissue: inhibitor sensitivity and environmental and hormonal regulation. J Exp Biol 180:163–174

Lin LY, Weng CF, Hwang PP (2001) Regulation of drinking rate in euryhaline tilapia larvae (*Oreochromis mossambicus*) during salinity challenges. Physiol Biochem Zool 74:171–177

Lorin-Nebel C, Avarre JC, Faivre N, Wallon S, Charmantier G, Durand JD (2012) Osmoregulatory strategies in natural populations of the black-chinned tilapia *Sarotherodon melanotheron* exposed to extreme salinities in West African estuaries. J Comp Physiol B 182:771–780

Malakpour Kolbadinezhad S, Coimbra J, Wilson JM (2018) Osmoregulation in the *Plotosidae* catfish: role of the salt secreting dendritic organ. Front Physiol 9:761–761

Marshall WS, Breves JP, Doohan EM, Tipsmark CK, Kelly SP, Robertson GN, Schulte PM (2018) claudin-10 isoform expression and cation selectivity change with salinity in salt-secreting epithelia of *Fundulus heteroclitus*. J Exp Biol 221:jeb168906

McCormick SD (1993) Methods for non-lethal biopsy and measurement of Na^+, K^+ ATPase activity. Can J Fish Aquat Sci 50:656–658

McDonald MD, Grosell M (2006) Maintaining osmotic balance with an aglomerular kidney. Comp Biochem Physiol A Mol Integr Physiol 143:447–458

Parmelee JT, Renfro JL (1983) Esophageal desalination of seawater in flounder: role of active sodium transport. Am J Physiol 245:R888-893

Pfaffl MW (2001) A new mathmatical model for relative quantification in real-time RT-PCR. Nucleic Acids Res 29:45

Rooker JR, Holt SA, Soto MA, Holt JG (1998) Postsettlement patterns of habitat use by sciaenid fishes in subtropical seagrass meadows. Estuaries 21:318–327

Rooker JR, Stunz GW, Holt SA, Minello TJ (2010) Population connectivity of red drum in the northern Gulf of Mexico. Mar Ecol Prog Ser 407:187–196

Sardella BA, Matey V, Cooper J, Gonzalez RJ, Brauner CJ (2004) Physiological, biochemical and morphological indicators of osmoregulatory stress in "California" Mozambique tilapia (*Oreochromis mossambicus* × *O. urolepis hornorum*) exposed to hypersaline water. J Exp Biol 207:1399–1413

Sattin G, Mager EM, Beltramini M, Grosell M (2010) Cytosolic carbonic anhydrase in the Gulf toadfish is important for tolerance to hypersalinity. Comp Biochem Physiol A Mol Integr Physiol 156:169–175

Schauer KL, Reddam A, Xu EG, Wolfe LM, Grosell M (2018) Interrogation of the Gulf toadfish intestinal proteome response to hypersalinity exposure provides insights into osmoregulatory mechanisms and regulation of carbonate mineral precipitation. Comp Biochem Physiol D 27:66–76

Scott GR, Baker DW, Schulte PM, Wood CM (2008) Physiological and molecular mechanisms of osmoregulatory plasticity in killifish after seawater transfer. J Exp Biol 211:2450–2459

Stunz GW, Minello TJ, Levin PS (2002) A comparison of early juvenile red drum densities among various habitat types in Galveston Bay, Texas. Estuaries 25:76–85

Taylor JR, Mager EM, Grosell M (2010) Basolateral NBCe1 plays a rate-limiting role in transepithelial intestinal HCO_3^- secretion, contributing to marine fish osmoregulation. J Exp Biol 213:459–468

Watson CJ, Nordi WM, Esbaugh AJ (2014) Osmoregulation and branchial plasticity after acute freshwater transfer in red drum, *Sciaenops ocellatus*. Comp Biochem Physiol A Mol Integr Physiol 178:82–89

Wilson SS, Dunton KH (2018) Hypersalinity during regional drought drives mass mortality of the seagrass Syringodium filiforme in a subtroical lagoon. Estuaries Coasts 41:855–865